

Quenched Averages for self-avoiding walks and polygons on deterministic fractals

Sumedha* and Deepak Dhar

*Department of Theoretical Physics, Tata Institute of Fundamental Research,
Homi Bhabha Road, Colaba, Mumbai 400005, India*

(Dated: November 13, 2018)

We study rooted self avoiding polygons and self avoiding walks on deterministic fractal lattices of finite ramification index. Different sites on such lattices are not equivalent, and the number of rooted open walks $W_n(S)$, and rooted self-avoiding polygons $P_n(S)$ of n steps depend on the root S . We use exact recursion equations on the fractal to determine the generating functions for $P_n(S)$, and $W_n(S)$ for an arbitrary point S on the lattice. These are used to compute the averages $\langle P_n(S) \rangle$, $\langle W_n(S) \rangle$, $\langle \log P_n(S) \rangle$ and $\langle \log W_n(S) \rangle$ over different positions of S . We find that the connectivity constant μ , and the radius of gyration exponent ν are the same for the annealed and quenched averages. However, $\langle \log P_n(S) \rangle \simeq n \log \mu + (\alpha_q - 2) \log n$, and $\langle \log W_n(S) \rangle \simeq n \log \mu + (\gamma_q - 1) \log n$, where the exponents α_q and γ_q take values different from the annealed case. These are expressed as the Lyapunov exponents of random product of finite-dimensional matrices. For the 3-simplex lattice, our numerical estimation gives $\alpha_q \simeq 0.72837 \pm 0.00001$; and $\gamma_q \simeq 1.37501 \pm 0.00003$, to be compared with the annealed values $\alpha_a = 0.73421$ and $\gamma_a = 1.37522$.

I. INTRODUCTION

Understanding the behavior of linear polymers in random media has been an important problem in statistical physics, both for reasons of theoretical interest, and applications. Calculation of quenched averages over the disorder is a very hard problem both analytically and computationally^{1,2}. There have been many speculations and controversies regarding critical behavior of self-avoiding walks (SAWs) in random media (especially at the percolation threshold). Exact calculation of quenched averages has not been possible so far for any nontrivial case, and simulations are not easy and often give contradicting results for this problem. In this context, it seems useful to construct a toy model, where one can explicitly calculate the quenched and annealed averages, and see their difference. This is what we shall do in this paper, for the problem of linear polymers on a deterministic fractal.

It is straight forward to calculate annealed averages of self-avoiding walks on deterministic fractals using real-space renormalization techniques^{3,4}. One can explicitly write down a closed set of exact renormalization equations in a finite number of variables, so long as the fractal has a finite ramification index. Then, the eigenvalues of the linearized recursion equations near the fixed point of the renormalization transformation determine the critical exponents of the problem. In fact, a good deal of understanding of the complex behavior of polymers with additional interactions, e.g. self-interaction, or with a wall, or with other polymers, has been obtained by studying the corresponding analytically tractable problem on fractals⁵.

It seems reasonable that the study of effect of inhomogeneities of the substrate would also be more tractable on fractal lattices. This is specially promising, as one does not need to introduce disorder in the problem from outside. The fractal lattices do not have translational symmetry, and hence a polymer living on a fractal lattice necessarily sees an inhomogeneous environment. Some regions of the lattice are better connected than others, and the local free density of the polymer per monomer in these regions would be lower than other parts. We want to understand the effect of presence of such regions on the large-scale structure and properties of the polymer. The main difference from the usual polymer in disordered medium problem to the case we study here is that the favorable and unfavorable regions are not randomly distributed over the lattice, but have a predetermined regular structure in the case of deterministic fractals. In this context, the annealed averages, which means averaging the partition function of the polymer over different positions, are appropriate in cases where the polymer can move freely over different parts of the lattice. The quenched average is averaging *the logarithm* of the partition function of the polymer over different positions, and would be appropriate where this freedom is not present.

The annealed average for linear and branched polymers have been calculated exactly for many different fractal lattices⁵. But to our knowledge the quenched averages have not been calculated so far on any fractal lattice. In this paper, we use the recursive structure of fractals to calculate quenched averages for linear polymers on deterministic

*Present address: Laboratoire de Physique Théorique et Modèles Statistiques, Université Paris-sud, F-91405, France

fractals. We find that the connectivity constant μ , and the radius of gyration exponent ν are the same for the annealed and quenched averages. The critical exponents for the quenched case can be expressed as the Lyapunov exponents for random product of finite-dimensional matrices. These can be estimated numerically efficiently by Monte Carlo methods, which we do for the illustrative case of 3-simplex fractal.

The rest of the paper is organized as follows: In section 2 we define the 3-simplex lattice and specify the scheme we use to label the sites of the lattice. We also define the annealed and quenched averages precisely, and the generating functions for different quantities of interest. In section 3 we work out the recursion equations for generating functions of self-avoiding polygons (SAPs) and SAWs on 3-simplex. In section 4 we derive rigorous bounds on the number of rooted SAPs and SAWs, and prove that the connectivity constant μ , and the size exponent ν are the same for the quenched and annealed averages. In section 5, we study the variation of the number of SAPs and SAWs with the position of the root on the 3-simplex lattice numerically. In section 6, we determine numerical values of the critical exponents in the quenched case by Monte Carlo determination of Lyapunov exponents for random products of matrices.

II. PRELIMINARIES AND DEFINITIONS

We will illustrate the general technique by working out explicitly the simple case of SAWs and SAPs on the 3-simplex fractal. The treatment is easily generalized to other recursively defined fractals of finite ramification index.

The 3-simplex graph is defined recursively as follows [Fig.1]: the graph of the first order triangle is a single vertex with 3 bonds. The $(r+1)$ th order triangle is formed by joining graphs of three r -th order triangle by connecting a dangling bond of each to a dangling bond of the other r th order subgraphs. There is one dangling bond left in each graph and 3 bonds altogether. In general, the r th order graph will have 3^{r-1} vertices and $(3^r - 3)/2$ internal bonds, and 3 boundary bonds. Clearly, the fractal dimension of this lattice is $\log 3 / \log 2$.

We use a ternary base single integer to label different sites of an r -th order triangle. The labeling is explained in Fig. 1. A point on the r -th order triangle is labelled by a string of $(r-1)$ characters, e.g. 0122201... Each character takes one of three values 0, 1 or 2. The leftmost character specifies in which of the three sub-triangles the point lies (0, 1 and 2 for the top, left and right sub-triangle respectively). The next character specifies placement in the $(r-1)$ -th order sub-triangle, and so on. On an infinite lattice, specification of S requires an infinitely long string. In discussing the local neighborhood of a site, we only need to know the last few digits of S . We will denote by $[S]_r$ the substring consisting of the last r characters of the integer label of S , and by s_r the r th digit in the string S counted from the right. As an example, for the string $S = 21...0112011$, $[S]_2 = 11$, and $s_3 = 0$. Also, in an obvious notation, $[S]_r = s_r[S]_{r-1}$.

The rooted polygons are polygons that pass through a given site (see Fig. 1) called the root. Let $P_n(S)$ be the number of rooted polygons of perimeter n corresponding to root S . The generating function for rooted polygons for root S is defined as

$$P(x; S) = \sum_{n=3}^{\infty} P_n(S) x^n \quad (1)$$

Similarly, we define $W_n(S)$ as the number of open walks of length n whose one end-point is S , and the corresponding generating function $W(x; S)$ by

$$W(x; S) = \sum_{n=1}^{\infty} W_n(S) x^n \quad (2)$$

For a given value of n , the values of $P_n(S)$ and $W_n(S)$ depend only on the last few digits in the ternary integer labeling S . For example, it is easy to check that if the last two digits of S are unequal, i.e. if $s_1 \neq s_2$ we have

$$P(x; S) = x^3 + x^6 + 3x^7 + 3x^8 + x^9 + \mathcal{O}(x^{12}). \quad (3)$$

But if $s_1 = s_2$

$$P(x; S) = x^3 + x^7 + 2x^8 + x^9 + \mathcal{O}(x^{12}) \quad (4)$$

In general, for any SAP configuration consisting of perimeter n , with $n < 3 \times 2^r$, with r an integer, one can find an $(r+1)$ -th order triangle graph, such that the polymer lies completely inside it. Then, the numbers $P_n(S)$ and

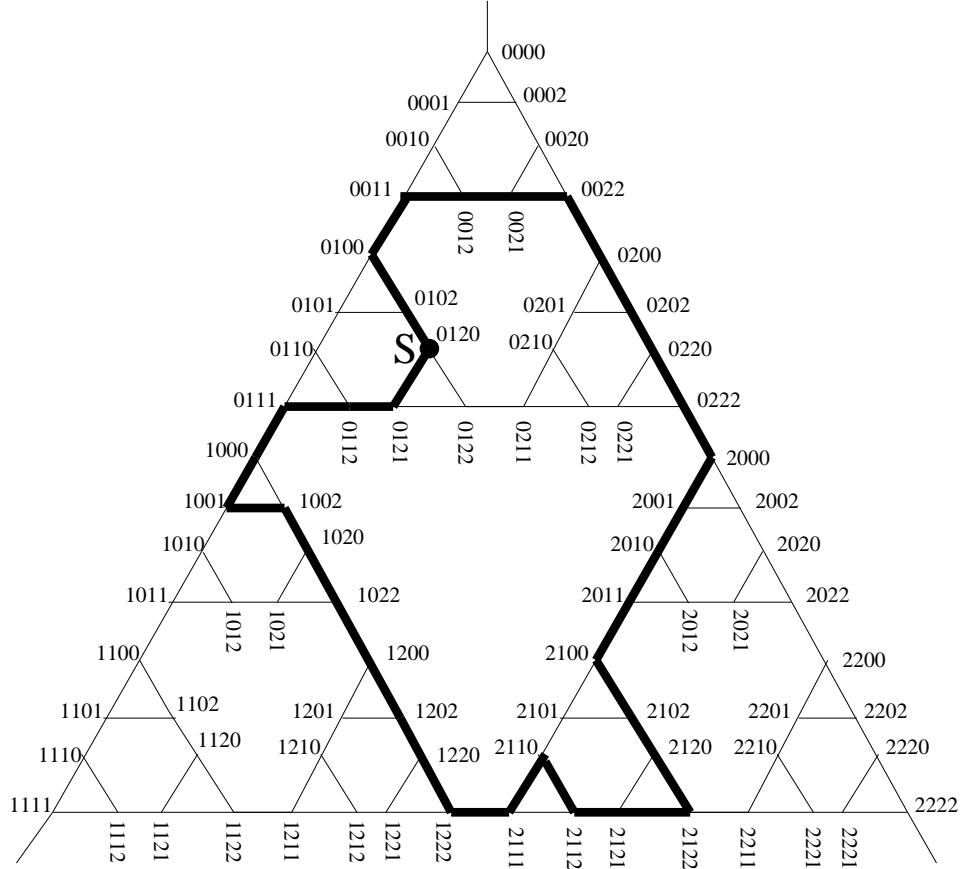


FIG. 1: The figure shows a 3 simplex graph of order 5, which is formed by joining 3 fourth order graphs. In general the r th order 3-simplex is formed by joining 3 graphs of $(r - 1)$ th order such that there is one dangling bond left in each subgraph. The thicker line shows a polygon of size 35 which passes through a particular site S .

$W_n(S)$ depend only the relative position of S within this triangle, and hence only on $[S]_r$. This then allows us to define averages of functions of $P_n(S)$ and $W_n(S)$. One assumes that S is equally likely to be any one of the 3^r sites in the $(r + 1)$ -th order triangle. So, for example, for $n = 7$, we have $r = 2$, and $P_7(S)$ depends only on $[S]_2$. Out of 9 possibilities for $[S]_2$, 3 have $s_1 = s_2$, and 6 cases have $s_1 \neq s_2$. Thus, if S is chosen at random, using Eq. (3-4), we have $\text{Prob}[P_7(S) = 3] = 2/3$, and $\text{Prob}[P_7(S) = 1] = 1/3$. We shall use angular brackets $\langle \rangle$ to denote averaging over different positions of the root S . This gives $\langle P_7 \rangle = 7/3$, and $\langle \log P_7 \rangle = \frac{2}{3} \log 3$. Other averages can be calculated similarly.

We shall call the values $\langle P_n(S) \rangle$, and $\langle W_n(S) \rangle$ as the annealed averages of $P_n(S)$ and $W_n(S)$, and define their generating functions

$$\bar{P}(x) = \sum_{n=3}^{\infty} \langle P_n(S) \rangle x^n \quad (5)$$

$$\bar{W}(x) = \sum_{n=1}^{\infty} \langle W_n(S) \rangle x^n \quad (6)$$

We define the growth constant μ_a , and the annealed exponents α_a and γ_a in terms of the behavior of $\langle P_n(S) \rangle$ and $\langle W_n(S) \rangle$ for large n :

$$\log \langle P_n(S) \rangle = n \log \mu_a + (\alpha_a - 2) \log n + \mathcal{O}(1) \quad (7)$$

$$\log \langle W_n(S) \rangle = n \log \mu_a + (\gamma_a - 1) \log n + \mathcal{O}(1) \quad (8)$$

It was shown in ref.3 that $\mu_a \approx 1.61803$, $\alpha_a \approx 0.73421$ and $\gamma_a \approx 1.37522$.

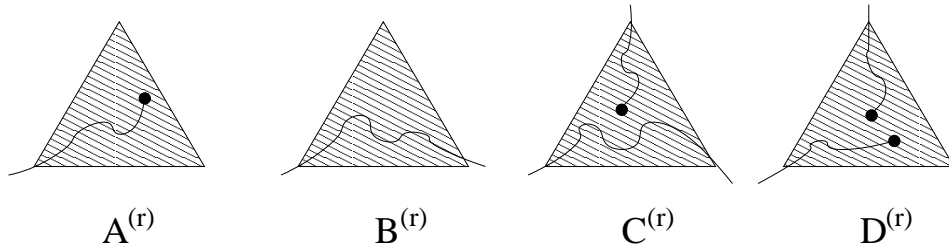


FIG. 2: Different restricted partition functions for the r th order triangle. Internal vertices inside the r th order triangle are not shown.

For the quenched averages, the exponents α_q and γ_q are defined by the condition that for large n

$$\langle \log P_n(S) \rangle = n \log \mu_q + (\alpha_q - 2) \log n + \mathcal{O}(1) \quad (9)$$

$$\langle \log W_n(S) \rangle = n \log \mu_q + (\gamma_q - 1) \log n + \mathcal{O}(1) \quad (10)$$

We define the order of a polygon as the order of the smallest triangular subgraph that contains all the sites occupied by the polygon. For defining the size exponent ν_a and ν_q , it is sufficient to adopt the simple definition that the diameter of a polygon is 2^r if its order is r . One can then define the mean diameter of all polygons of perimeter n rooted at a given site S , as the average diameter, with all such polygons given equal weight. We define the quenched average mean diameter as the average over different positions of S of the average diameter of polygons of perimeter n rooted at S . The size-exponent ν_q for quenched averages is defined by the condition that the quenched average diameter varies as n^{ν_q} for large n .

To define the annealed average for the diameter of SAP of perimeter n , we assign equal weight to all such loops within an s th order triangle with $2^s > n$, and calculate the average diameter. It is easy to see that the answer does not depend on s . Again, we define the annealed size exponent ν_a by the condition that the annealed average diameter varies as n^{ν_a} for large n .

The exponents for open walks can be defined similarly. We shall argue that the size exponents for open walks and polygons are the same, and further that $\mu_q = \mu_a$, and $\nu_q = \nu_a$, and hence simply write μ and ν without any subscript, if the distinction is unnecessary.

Note that we have to first average over different positions of the root for a fixed n , and then let n tend to infinity to define ν_q . If we take the large n limit first, for a fixed position of the root, then even the convergence of large n limit of $\log[P_n(S)\mu^{-n}]/\log n$ and $\log[W_n(S)\mu^{-n}]/\log n$ is not obvious due to the irregular variation of $\log P_n(S)$ and $\log W_n(S)$ with n . The amount of fluctuations in different averages of observables over different positions of the root will be discussed in section 5.

III. THE RENORMALIZATION EQUATIONS

In this section, we briefly recapitulate the renormalization scheme for calculating the annealed averages used in ref. 3, and then adapt it for calculating properties of rooted walks.

Consider one r -th order triangular subgraph of the infinite order graph. It is connected to the rest of the lattice by only three bonds. Our aim is to sum over different configurations of the SAW that lie within the subgraph, with a weight x for each step of the walk. These configurations can be divided into four classes, as shown in Fig. 2, and we define four restricted partition functions $A^{(r)}$, $B^{(r)}$, $C^{(r)}$ and $D^{(r)}$ corresponding to these four classes.

Here $A^{(r)}$ is the sum over all configurations of the walk within the r -th order triangle, that enters the triangle from a specified corner, and with one endpoint inside the triangle. $B^{(r)}$ is the sum over all configurations of walk within the triangle that enters and leaves the triangle from specified corner vertices. $C^{(r)}$ and $D^{(r)}$ are defined similarly (Fig. 2). For any given value of r , $B^{(r)}$, $D^{(r)}$, $A^{(r)}\sqrt{x}$, $C^{(r)}\sqrt{x}$ are finite degree polynomials in x with non-negative integer coefficients. It is easy to see that the starting values of these variables are

$$A^{(1)} = \sqrt{x}, \quad B^{(1)} = x, \quad C^{(1)} = D^{(1)} = 0. \quad (11)$$

We note the generating function for $\bar{P}(x)$ is simply related to the generating function of unrooted polygons $P_{nroot}(x)$ by the relation $\bar{P}(x) = x \frac{d}{dx} P_{nroot}(x)$. The sum over all unrooted polygons of order $(r+1)$ within an $(r+1)$ -th order

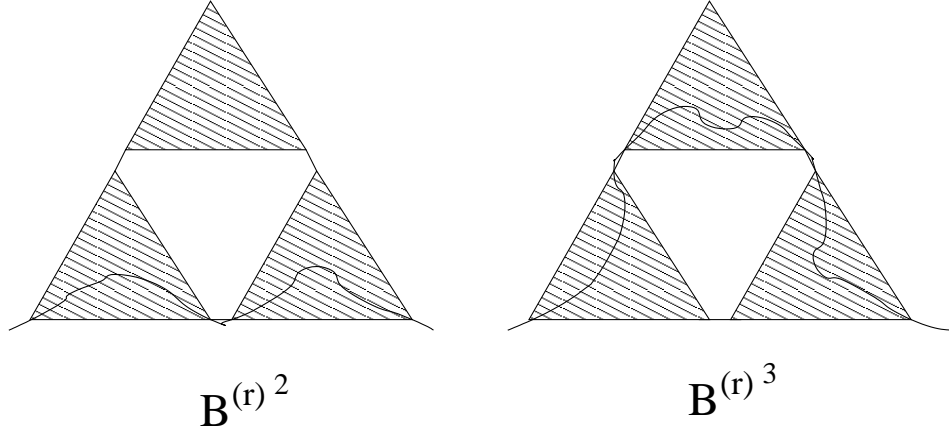


FIG. 3: Two possible ways of getting a polymer configuration of type B

triangle is $B^{(r)3}$, and number of sites in the $(r+1)$ -th order triangle is 3^r , hence we get

$$P_{noroot}(x) = \sum_{r=1}^{\infty} 3^{-r} B^{(r)3}. \quad (12)$$

here we have suppressed the x dependence of B . In rest of the paper, we will suppress the x -dependence of variables A, B, C, D , to simplify notation, whenever the meaning is clear from the context.

The sum over unrooted open walks can be expressed similarly

$$W_{noroot}(x) = \sum_{r=1}^{\infty} 3^{-r} [3A^{(r)2} + 3B^{(r)}A^{(r)2} + 3B^{(r)2}D^{(r)}]. \quad (13)$$

It is straight forward to write down the recursion equations for these weights $A^{(r+1)}, B^{(r+1)}, C^{(r+1)}$ and $D^{(r+1)}$ in terms of the weights at order r . For example, Fig. 3 shows the only two possible ways one can construct a polymer configuration of type B .

$$B^{(r+1)} = B^{(r)2} + B^{(r)3}. \quad (14)$$

Similarly, we get

$$\begin{pmatrix} A^{(r+1)} \\ C^{(r+1)} \end{pmatrix} = \begin{pmatrix} 1 + 2B^{(r)} + 2B^{(r)2} & 2B^{(r)2} \\ B^{(r)2} & 3B^{(r)2} \end{pmatrix} \begin{pmatrix} A^{(r)} \\ C^{(r)} \end{pmatrix} \quad (15)$$

and

$$\begin{aligned} D^{(r+1)} = & A^{(r)2} + 2A^{(r)2}B^{(r)} + 4A^{(r)}B^{(r)}C^{(r)} \\ & + 6B^{(r)}C^{(r)2} + D^{(r)}(2B^{(r)} + 3B^{(r)2}) \end{aligned} \quad (16)$$

We note that the equation (14) has one nontrivial fixed point $B = B^* = \frac{\sqrt{5}-1}{2}$. For starting value $x < B^*$, the recursions give $B^{(r)} \rightarrow 0$ as r tends to infinity, but for $x > B^*$, $B^{(r)}$ increases to infinity for large r . This gives the connectivity constant $\mu = 1/B^* = (\sqrt{5}+1)/2$, the golden mean. Linearizing the recursion equation about this nontrivial fixed point, we see that deviations from the fixed point value increases as $B^{(r+1)} - B^* \approx \lambda_1(B^{(r)} - B^*)$, with $\lambda_1 = 2 + \mu^{-2}$. This then implies³ that $\nu_a = \log 2 / \log \lambda_1 \approx 0.79862$.

The critical exponent γ is determined in terms of the larger eigenvalue λ_2 of the 2×2 matrix in Eq. 15 evaluated at the non-trivial fixed point³, $(A^*, B^*, C^*) = (0, 1/\mu, 0)$. We get

$$\gamma_a = \frac{\log(\lambda_2^2/3)}{\log \lambda_1} \approx 1.37522. \quad (17)$$

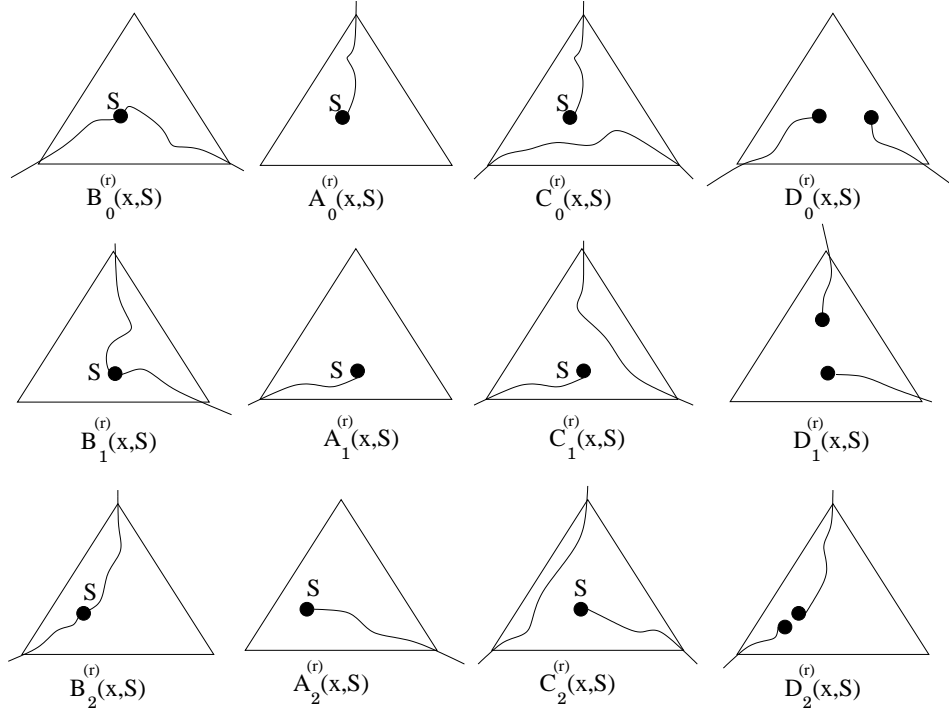


FIG. 4: Definition of weights for rooted graphs. In case of D , S can be any of the two end-points of the walk (shown by filled circles in the figure).

The recursion equations for rooted SAP's and SAW's are constructed similarly. We define $B_s^{(r)}(S)$ for $s = 0, 1$ and 2 as the sum over walks on the r th order triangle that go through two corners of the triangle, visit the site S , avoiding the top, left and right corners for $s = 0, 1$ and 2 respectively (Fig 4). Since $B_s^{(r)}(S)$ depends on S only through $[S]_{r-1}$, we shall write $B_s^{(r)}(S) = B_s^{(r)}([S]_{r-1})$. For any given r and S , these are finite degree polynomials in x . Similarly, we have to define three functions $A_s^{(r)}([S]_{r-1})$ and $C_s^{(r)}([S]_{r-1})$ for $s = 0, 1, 2$ instead of the single variables A , C and D for the unrooted problem, as the root breaks the symmetry between the corner sites of the r -th order triangle (Fig. 4).

A site in the $(r+1)$ -th order triangle is characterized by a string of r characters. Hence, a site characterized by string S at the r -th stage will be characterized by one of the strings $0S$, $1S$ or $2S$ at $(r+1)$ th stage.

We can now write the recursions similar to Eq. 14 for $B_s^{(r+1)}([S]_r)$, for $s = 0, 1$ and 2 in terms of weights of r th order graphs. For example, one can construct $B_0^{(r+1)}(0S)$ in just one way as shown in Fig. 5. The recursion relation for $B_0^{(r+1)}([S]_r)$ will be

$$B_0^{(r+1)}(0[S]_{r-1}) = (B^{(r)})^2 B_0^{(r)}([S]_{r-1}) \quad (18)$$

Clearly, all the recursion relations for rooted polygons are linear in the rooted restricted partition functions of lower order $B_s^{(r)}([S]_{r-1})$, and can be written in the matrix form. With $[S]_r = s_r[S]_{r-1}$, we have

$$\begin{pmatrix} B_0^{(r+1)}([S]_r) \\ B_1^{(r+1)}([S]_r) \\ B_2^{(r+1)}([S]_r) \end{pmatrix} = \mathcal{M}_{s_r} \begin{pmatrix} B_0^{(r)}([S]_{r-1}) \\ B_1^{(r)}([S]_{r-1}) \\ B_2^{(r)}([S]_{r-1}) \end{pmatrix} \quad (19)$$

where

$$\mathcal{M}_0 = \begin{pmatrix} B^2 & 0 & 0 \\ 0 & B & B^2 \\ 0 & B^2 & B \end{pmatrix}; \quad \mathcal{M}_1 = \begin{pmatrix} B & 0 & B^2 \\ 0 & B^2 & 0 \\ B^2 & 0 & B \end{pmatrix};$$

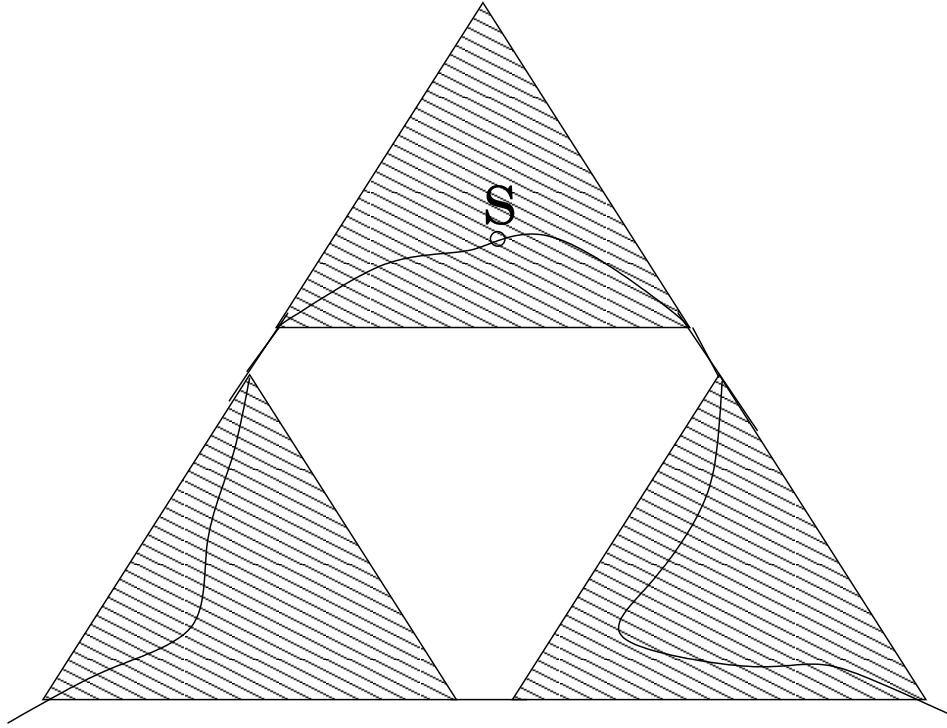


FIG. 5: The only configurations contributing to $B_0^{(r+1)}(x, 0S)$. Here each sub-triangle is a r^{th} order 3-simplex.

$$\mathcal{M}_2 = \begin{pmatrix} B & B^2 & 0 \\ B^2 & B & 0 \\ 0 & 0 & B^2 \end{pmatrix}. \quad (20)$$

Here we have suppressed the superscript (r) of B in the matrices \mathcal{M}_0 , \mathcal{M}_1 and \mathcal{M}_2 . The generating function for rooted polygons, rooted at a site S is given by

$$P(x, S) = \sum_{r=1}^{\infty} B_{s_r}^{(r)}([S]_{r-1}) B^{(r)^2} \quad (21)$$

Similarly, we can write the recursion equations for $A_s^{(r)}([S]_{r-1})$ and $C_s^{(r)}([S]_{r-1})$ and $D_s^{(r)}([S]_{r-1})$ defined analogous to $B_s^{(r)}([S]_{r-1})$, with $s = 0, 1$, or 2 . The A 's and C 's depend on each other and the recursion relations for them are

$$\begin{pmatrix} A_0^{(r+1)}([S]_r) \\ A_1^{(r+1)}([S]_r) \\ A_2^{(r+1)}([S]_r) \\ C_0^{(r+1)}([S]_r) \\ C_1^{(r+1)}([S]_r) \\ C_2^{(r+1)}([S]_r) \end{pmatrix} = \mathcal{L}_{s_r} \begin{pmatrix} A_0^{(r)}([S]_{r-1}) \\ A_1^{(r)}([S]_{r-1}) \\ A_2^{(r)}([S]_{r-1}) \\ C_0^{(r)}([S]_{r-1}) \\ C_1^{(r)}([S]_{r-1}) \\ C_2^{(r)}([S]_{r-1}) \end{pmatrix} \quad (22)$$

where

$$\mathcal{L}_0 = \begin{pmatrix} 1 & 0 & 0 & 0 & B^2 & B^2 \\ 0 & B & B^2 & 0 & 0 & 0 \\ 0 & B^2 & B & 0 & 0 & 0 \\ B^2 & 0 & 0 & B^2 & 0 & 0 \\ 0 & 0 & 0 & 0 & B^2 & 0 \\ 0 & 0 & 0 & 0 & 0 & B^2 \end{pmatrix};$$

$$\mathcal{L}_1 = \begin{pmatrix} B & 0 & B^2 & 0 & 0 & 0 \\ 0 & 1 & 0 & B^2 & 0 & B^2 \\ B^2 & 0 & B & 0 & 0 & 0 \\ 0 & 0 & 0 & B^2 & 0 & 0 \\ 0 & B^2 & 0 & 0 & B^2 & 0 \\ 0 & 0 & 0 & 0 & 0 & B^2 \end{pmatrix};$$

$$\mathcal{L}_2 = \begin{pmatrix} B & B^2 & 0 & 0 & 0 & 0 \\ B^2 & B & 0 & 0 & 0 & 0 \\ 0 & 0 & 1 & B^2 & B^2 & 0 \\ 0 & 0 & 0 & B^2 & 0 & 0 \\ 0 & 0 & 0 & 0 & B^2 & 0 \\ 0 & 0 & B^2 & 0 & 0 & B^2 \end{pmatrix} \quad (23)$$

Here again we have suppressed the superscript (r) on the B 's. One can now write similar recursion for $D^{(r)}([S]_r)$ also. [Like the annealed case³, these variables are not needed for the determination of critical exponents, though they are needed to determine $W_n(S)$.] Here we write down the recursions for $D_0^{(r+1)}([S]_r)$. similar relations will hold for $D_1^{(r+1)}([S]_r)$ and $D_2^{(r+1)}([S]_r)$.

$$\begin{aligned} D_0^{(r+1)}(0[S]_{r-1}) &= (AB + 2BC)(A_1 + A_2) + B^2 D_0 \\ D_0^{(r+1)}(1[S]_{r-1}) &= (A + AB)A_1 + (AB + 2BC)(C_1 + C_2) \\ &\quad + D_0 B + D_2 B^2 + 2BCC_0 \\ D_0^{(r+1)}(2[S]_{r-1}) &= (A + AB)A_2 + (AB + 2BC)(C_1 + C_2) \\ &\quad + D_0 B + D_1 B^2 + 2BCC_0 \end{aligned} \quad (24)$$

where we have suppressed the $([S]_{r-1})$ dependence, and the superscripts (r) in the terms on the right hand side.

We can also express the open walks generating function $W(x, S)$ in terms of these restricted partition functions. It is easy to show that

$$\begin{aligned} W(x; S) &= \sum_{r=1}^m \left[\sum_{s' \neq s_r} A_{s'}([S]_{r-1})(A + AB) + D_{s_r}([S]_{r-1})B^2 \right] \\ &\quad + AA_{s_m}([S]_{m-1}) + \mathcal{O}(x^{2^{m-1}}) \end{aligned} \quad (25)$$

In the limit of large m , the last term can be dropped, and we get

$$W(x; S) = \sum_{r=1}^{r=\infty} \left[\sum_{s' \neq s_r} A_{s'}([S]_{r-1})(A + AB) + D_{s_r}([S]_{r-1})B^2 \right] \quad (26)$$

For order r , there are 3^{r-1} different choices for $[S]_{r-1}$, and 3 choices of s each of the A_s, B_s, C_s and D_s , a total of $4 \cdot 3^r$ polynomials. The generating function for walks rooted at one end $W(x, S)$ can be easily written in terms of these generating functions. To determine $P(x, S)$ and $W(x, S)$ to given order n in x , we need to determine these only upto a finite order r . Thus, we have an efficient algorithm to explicitly determine these polynomials to any given order, and also to calculate the different averages over different sites. The explicit enumeration of rooted walks on fractals was studied by Reis⁷ and Ordemann et. al⁸, but the sizes they could reach were much smaller. We have obtained exact values of SAWs upto length 128 and SAPs upto 768 for all sites of the fractal, using our recursion equations (see Table.1)

IV. DETERMINATION OF THE GROWTH CONSTANT

We note that the recursion equation of $B^{(r)}$ (Eq. 14) does not involve the rooted variables $B_s^{(r)}(S)$, but not vice versa. If we start with a value $x < B^* = 1/\mu$, then for large r , $B^{(r)}$ tends to zero. This would make the rooted variables $B_s^{(r)}(S)$ also tend to zero for large r . However, if $x > B^*$, then $B^{(r)}$ will diverge for large r , and this would make $B_s^{(r)}(S)$ also diverge for all S . Thus we conclude that for all S , $P(x, S)$ and $W(x, S)$ converge if $x < 1/\mu$, and diverge if $x > 1/\mu$. Hence it follows that the critical growth constant is μ , for all S .

Consider now polygons or walks of finite length n , with n large. We think of x as the fugacity variable for each step. Then large n corresponds to initial value x very near $1/\mu$, say $x = 1/\mu - \delta$ where δ scales as $1/n$. Under renormalization, the value of $B^* - B^{(r)}$ increases, and there is a value r_0 such that for $r - r_0 \gg 1$, $B^{(r)} \approx 0$, and for $r_0 - r \gg 1$, $B^{(r)} \approx B^*$. Then, the recursion equations 19 and 22 imply that the rooted partition functions $B_s^{(r)}(S)$ and $C_s^{(r)}(S)$ also become very small for $r > r_0$, while $A_s^{(r)}$ tends to a finite value as r tends to infinity. The value of r_0 increases as δ is decreased as $r_0 \approx \frac{\log(1/\delta)}{\log \lambda_1}$, and the diameter of polymer increases as $2^{r_0} \sim \delta^{-\nu_a}$. As $\delta \sim 1/n$, this implies that the average size of polymer increases as n^ν , independent of S , and hence $\nu_q = \nu_a$.

An alternative proof of the assertion that the growth constant μ is the same for all sites is provided by setting up upper and lower bounds for $P_n(S)$ and $W_n(S)$, which have the same exponential growth.

We first obtain an upper bound on $P_n(S)$. If we ignore the constraint that the walk has to pass through S , we get an upper bound on the number of such walks. For example, for walks contributing to $B^{(r)}(S)$ we can write $B_\sigma^{(r)}(x, S) \leq B^{(r)}(x)$ where $\sigma = 0, 1, 2$ and the inequality between polynomials is understood to imply inequality for the coefficient of each power of x . This implies that for all sites S ,

$$P(x, S) \leq \sum_{r=1}^{\infty} B^{(r)} x^3 \quad (27)$$

If we write the function giving the upper bound in right-hand-side as $U(x)$, then $U(x)$ satisfies the equation

$$U(x) = x^3 + U(x^2 + x^3) \quad (28)$$

This functional equation again has the fixed point at $x^* = 1/\mu$, and linear analysis near the fixed point shows that $U(x)$ diverges as $-\log(1 - x\mu)$ as x tends to $1/\mu$ from below. This implies that the coefficient of x^n in the Taylor expansion of $U(x)$ varies as μ^n/n for large n . Thus,

$$P_n(S) \leq K\mu^n/n, \text{ for all } n, \text{ and all } S, \quad (29)$$

where K is some constant.

We now obtain a lower bound for $P_n(S)$. Let S_0 be the site whose label is a string with all digits 0. This is the topmost site of the triangular graph. For such a site $B_0^{(r)}(x; S_0)$ satisfies the following recursion

$$B_0^{(r)}(S_0) = (B^{(r-1)})^2 B_0^{(r-1)}(S_0) \quad (30)$$

Clearly, for all sites S , we have $B_0^{(1)}(S) \geq B_0^{(1)}(S_0)$. Then, using Eq.(18) and (19), by mathematical induction, we see that for all r, s and S

$$B_s^{(r)}(S) \geq B_0^{(r)}(S_0), \text{ for } s = 0, 1, 2. \quad (31)$$

This implies for any site S

$$P(x, S) \geq P(x, S_0) = \sum_{r=1}^{\infty} B^{(r)^2} B_0^{(r)}(S_0) \quad (32)$$

Clearly, the lower bound is actually attained for $S = S_0$. If we take $P(x, S_0) = xL(x)$, then $L(x)$ satisfies the following equation

$$L(x) = x^2 + x^2 L(x^2 + x^3) \quad (33)$$

Assuming that $L(x)$ near $x = 1/\mu$ has a singular expansion of the form $L(1/\mu - \delta) = L(1/\mu) - K\delta^b$, where K is some constant, we get

$$b = 2 \log \mu / \log(2 + \mu^{-2}) = 0.92717 \quad (34)$$

and hence

$$P_n(S) \geq K_1 \mu^n n^{-b-1} \quad (35)$$

where K_1 is a constant. Hence for any S , we have proved

$$K_1 \mu^n n^{-b-1} \leq P_n(S) \leq K \mu^n / n \quad (36)$$

Thus, in the limit of large n , for all sites S , we must have

$$\lim_{n \rightarrow \infty} \frac{\log P_n(S)}{n} = \mu \quad (37)$$

We also get the nontrivial bounds

$$1 - b \leq \alpha_q \leq 1 \quad (38)$$

Similarly it is easy to prove upper and lower bounds for open walks. A simple lower bound is provided by the inequality $W_n(S) \geq P_n(S)$, for all S . An upper bound to $\langle \log W_n(S) \rangle$ is provided by $\log \langle W_n(S) \rangle$. But the latter is known to vary as $n \log \mu + (\gamma_a - 1) \log n$ for large n . Hence we get

$$\lim_{n \rightarrow \infty} \frac{1}{n} \langle \log W_n(S) \rangle = \mu. \quad (39)$$

V. VARIATION OF $P_n(S)$ AND $W_n(S)$ WITH S AND n

We use the recursion equations (19-25) to calculate the values of $P_n(S)$ and $W_n(S)$ for different choices of the root S . For an SAP of order r , the minimum perimeter is $3 \times 2^{r-2}$. We could study these recursions upto $r = 9$ and hence took into account all self avoiding polygons upto sizes $n = 3 \times 2^8 = 768$. A 9-th order triangle has $3^8 = 6561$ vertices. we calculated the different polynomials $A_s(S)$, $B_s(S)$, $C_s(S)$ and $D_s(S)$ for $s = 0, 1, 2$ and 3^8 possible values of S , keeping all terms up to order x^{768} in each polynomial. The coefficients for large order become rather large. For example, the number of polygons of size 768 for the topmost site of the fractal graph is $\approx 2.5 \times 10^{154}$. We used the symbol manipulation software Mathematica⁶, which allows one to work with integers of arbitrary size. These then are used to calculate various averages.

In Fig. 6, we have shown the variation of $P_n(S)\mu^{-n}$ with n for some selected values of S . We see clearly roughly log-periodic variation in these numbers. We have also plotted the upper and lower bounds on $P_n(S)$ derived [Eq.(27 and 32)]. As was argued there, there is a site S_0 which saturates the lower bound. However, there is no single site that saturates the upper bound. Most of the polygons having a given value of perimeter n , have a particular order r , and have to pass through the three bonds joining the $(r-1)$ -order subgraphs. The six sites that are at the ends of these bonds clearly maximize $P_n(S)$. The sites change if n changes to correspond to polygons with one higher order.

In Fig. 7, we show the variation of exactly calculated values of $\log \langle P_n(S) \rangle$ and $\langle \log P_n(S) \rangle$ with n . We also show the maximum and minimum values of $\log P_n(S)$ attained, as a function of n , as S takes all possible values. Note that though we could study sizes upto 768 exactly, it is difficult to estimate α_a and α_q even to two digit precision from the data using standard series extrapolation techniques because of log-periodic oscillations.

The log-periodic variation of P_n is easy to understand qualitatively^{9,10}. All SAP's of order r in a given $(r+1)$ th order triangle have to pass through the three constriction points where the constituting r -th order triangles are joined. There is a natural length $n \sim C\lambda_1^r$, where C is some constant, for a polymer that does this. If the length is somewhat smaller than this value, the polymer is a bit stretched, and has a lower entropy. If it is a higher by a factor 1.5 or so, it loses entropy as many monomers have to squeeze in the same space. If the value of n increases by a factor λ_1 , then same thing happens at a higher order triangle. The sites which maximize $P_n(S)$ for a given n are the at the constriction points of the the corresponding r -th order triangles. As $\log n$ changes, these points also change. The fractional number of points S for which $P_n(S)$ attains its maximum value clearly varies as 3^{-r} , where r is the order

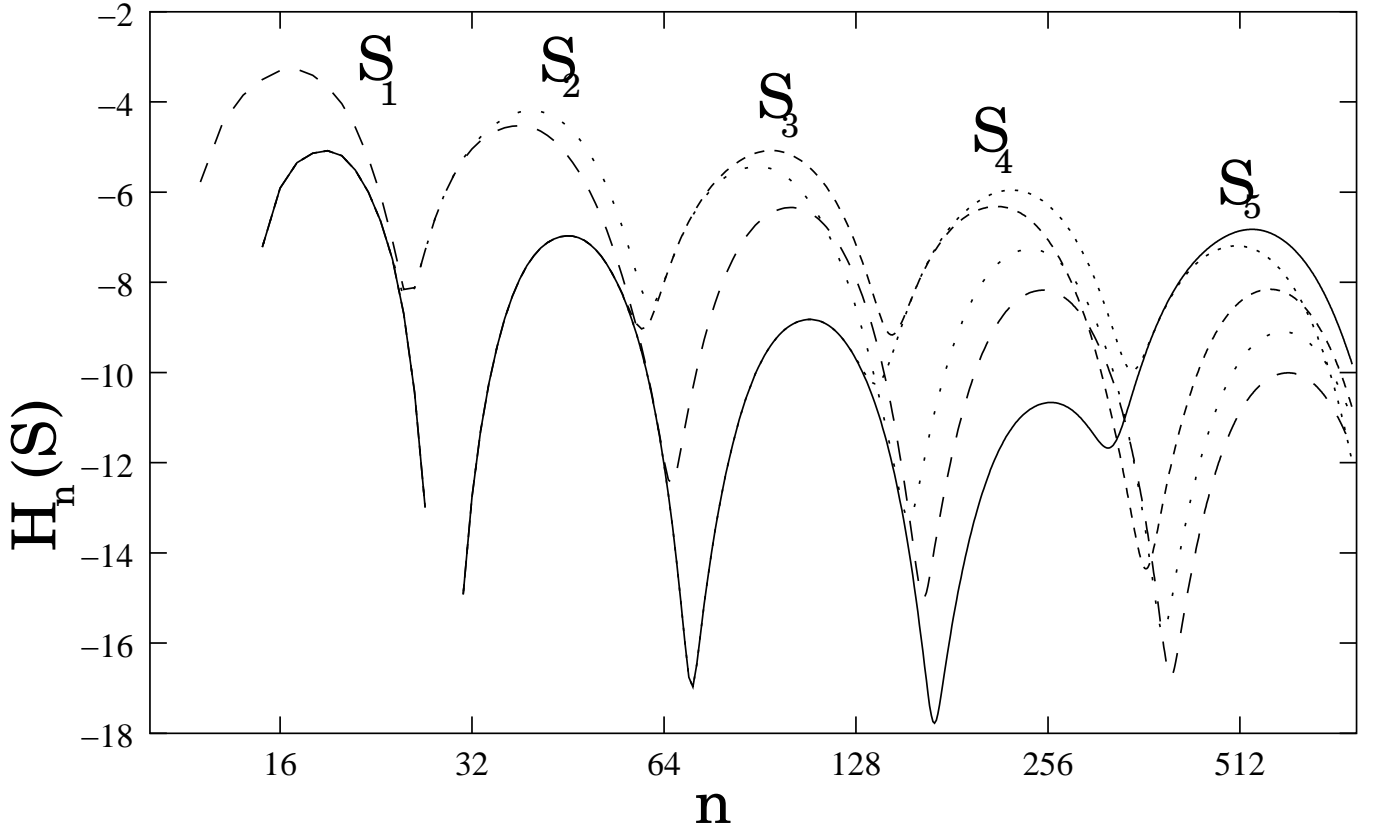


FIG. 6: Figure shows $H_n(S) = \log P_n(S) \mu^{-n}$ plotted as a function of n for five different values of S . These S are chosen near the constriction points and hence they maximize $P_n(S)$ for a given n . Here $S_1 = 00000211, S_2 = 00002111, S_3 = 00021111, S_4 = 00211111$ and $S_5 = 02111111$. Each of these values of S attains the maximum for some range of n . The points, defined only for integer n , have been joined by straight-line segments as an aid to the eye.

of a typical loop of perimeter n . Using $n \sim R^{1/\nu}$, we see that the density of points varies as $R^{-D} \sim n^{-D/\nu}$, where $d = \log 3 / \log 2$ is the fractal dimension of the lattice.

The log-periodic oscillations for open walks are much smaller in magnitude than in case of polygons. Here also, the number of open walks of order r is greater if the root is near the corner point of an r^{th} order triangle, as then it gets more space to explore and hence more entropy. We find the amplitude of oscillations in H_n is approximately 100 times smaller than for the corresponding quantity for closed polygons shown in Fig. 6 and 7. In Fig. 8 we show the exact values quenched and annealed averages for walks upto size 128. The difference in the two averages in the case of walks is smaller than for the polygons.

In Figs. 9 and 10 we have shown the density plots for SAPs on fractal lattices for $n = 400$ and $n = 600$. The different sites are shown by different colours depending on the value of $\log P_n$ at that site. The blue regions represent sites with largest values of $P_n(S)$. We clearly see that depending on value of n some sites are more favoured than others. We note that the difference between maximum and minimum values of $\log P_n(S)$ is more than 10 for $n = 400$, but only about half of this value for $n = 600$.

VI. CALCULATION OF EXPONENTS FOR QUENCHED AVERAGES

We note that to a very good approximation, all loops of a given perimeter n have the same order, say r_0 , where r_0 is an integer approximately equal to $\frac{\log n}{\log \lambda_1}$. The contribution of these loops to $P(x; S)$ then comes mostly from the single term $T_{r_0} = B_{s_{r_0}}^{(r_0)}([S]_{r_0-1}) B^{(r_0)^2}$ corresponding to $r = r_0$ in the equation (21). Also, if $x = 1/\mu = B^*$, then the contribution is $P_n(S) \mu^{-n}$, which is a slowly varying function of n . The contribution of nearby values of n to the r_0 -th

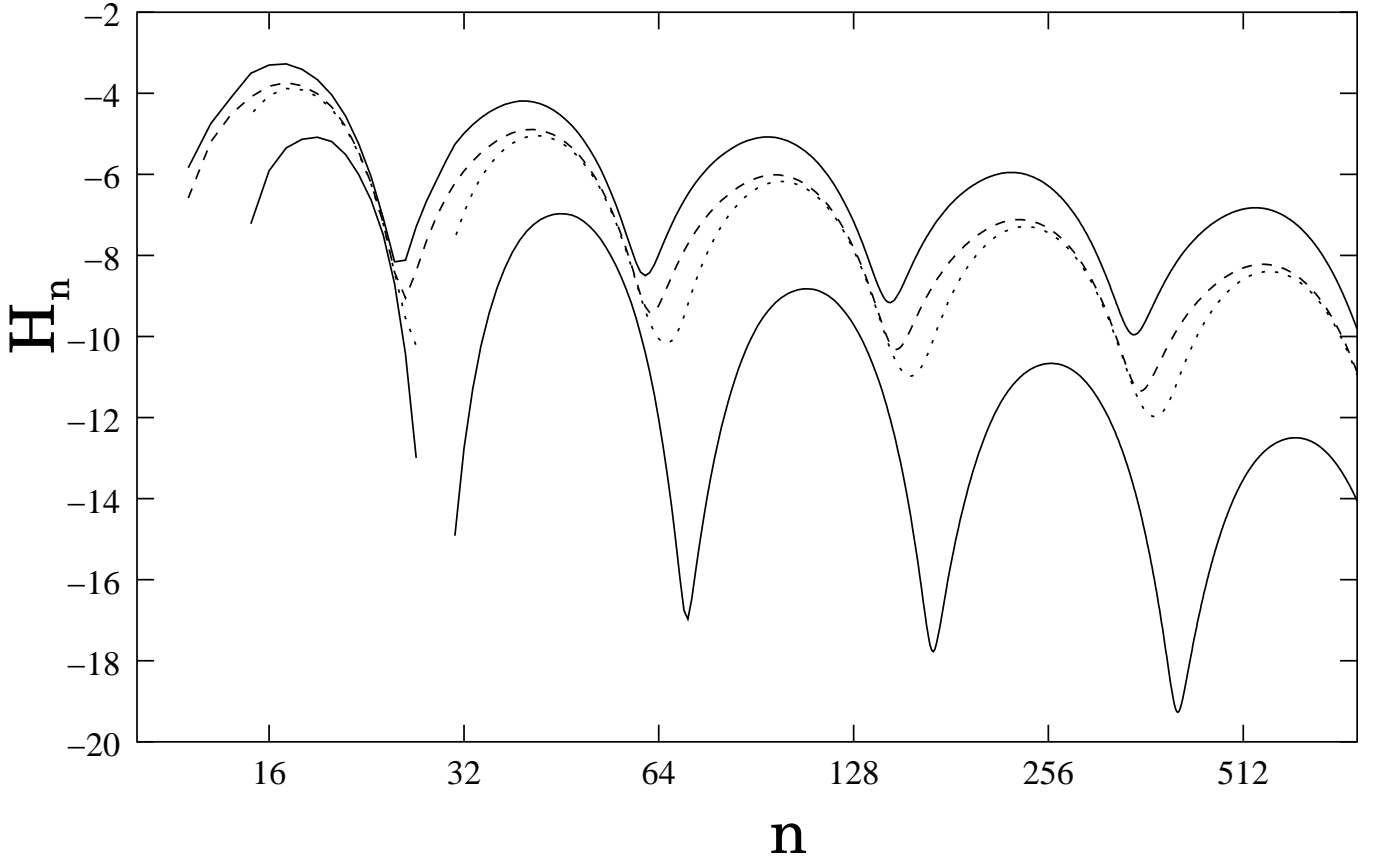


FIG. 7: A plot of average value of $\log P_n(S) \mu^{-n}$ (H_n) as a function of n . The uppermost and the lowermost curves are theoretically derived upper and lower bounds to this number over different positions. The dashed and dotted lines show the annealed and quenched average value respectively.

term will be comparable. The number of such terms that contribute to the r_0 -th term is of order n . Thus we have,

$$P_n(S) \mu^{-n} \sim \frac{1}{n} T_{r_0}(S) \quad (40)$$

For $x = B^*$, the matrices $\mathcal{M}_0, \mathcal{M}_1, \mathcal{M}_2$ become independent of r , and T_{r_0} is of the form

$$T_{r_0} = \langle v_1 | \mathcal{M}_{s_{r-1}} \dots \mathcal{M}_{s_4} \mathcal{M}_{s_3} \mathcal{M}_{s_2} \mathcal{M}_{s_1} | v_2 \rangle \quad (41)$$

Here $\langle v_1 |$ and $| v_2 \rangle$ are specific 3-dimensional bra- and ket vectors. Then from the general theory of random product of matrices^{11,12,13}, it follows that the probability distribution of T_{r_0} tends to a log-normal distribution for large r_0 , and

$$\lim_{r_0 \rightarrow \infty} \frac{1}{r_0} \log T_{r_0} = \log \Lambda_1 \quad (42)$$

where $\log \Lambda_1$ is the largest Lyapunov exponent for the random product of matrices. This also implies that the variance of $\log P_n(S)$ will be proportional to $\log n$. This is much less than some positive power of n , which is the expected behaviour for the usual polymer in the random medium problem. For example, for the directed polymer in a random medium, the variance of free energy of an n monomer chain varies as $n^{2/3}$. This is due to the fact that in the deterministic fractal case studied here, the favourable and unfavourable regions are very evenly distributed.

It then follows that $\langle \log[P_n(S) \mu^{-n}] \rangle$ tends to $r_0 \log \Lambda_1 - \log n$. Putting $r_0 \approx (\log n)/(\log \lambda_1)$, we get

$$\alpha_q = 1 + \log \Lambda_1 / \log \lambda_1 \quad (43)$$

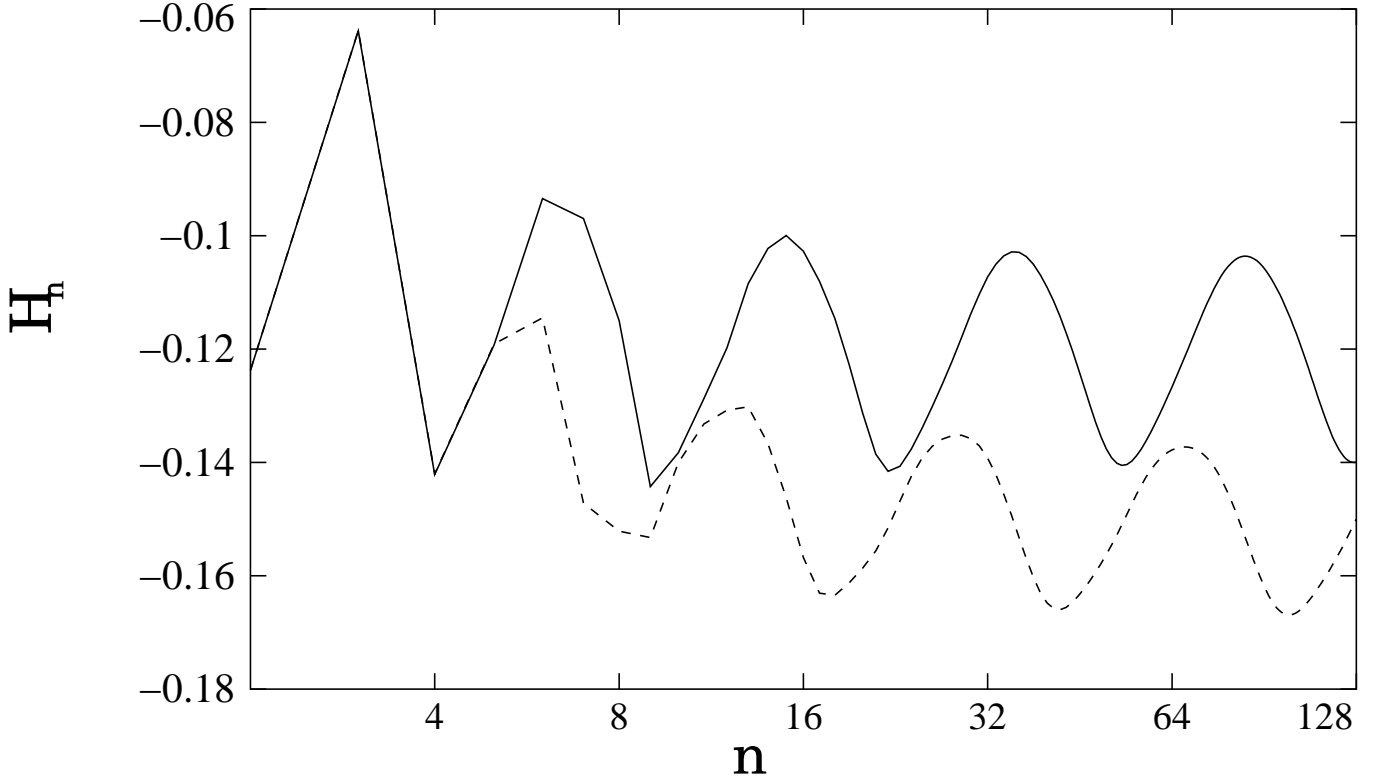


FIG. 8: The figure shows plots of $H_n = \log \langle W_n(S) \rangle - C_n$ (solid line) and $\langle \log W_n(S) \rangle - C_n$ (dotted line), where $C_n = n \log \mu + (\gamma_a - 1) \log n$.

It is straightforward to estimate Λ_1 numerically. We start with an arbitrary initial 3-dimensional vector $|v_0\rangle$ of positive elements with sum 1, and evolve it randomly by the rule

$$|v_{j+1}\rangle = a_j M_j |v_j\rangle \quad (44)$$

where M_j is randomly chosen to be one of three matrices M_0, M_1, M_2 and a_j is a multiplying factor chosen so that the sum of elements of new vector is again 1. The M_j are

$$\begin{aligned} M_0 &= \begin{pmatrix} B^{*2} & 0 & 0 \\ 0 & B^* & B^{*2} \\ 0 & B^{*2} & B^* \end{pmatrix}; \\ M_1 &= \begin{pmatrix} B^* & 0 & B^{*2} \\ 0 & B^{*2} & 0 \\ B^{*2} & 0 & B^* \end{pmatrix}; \\ M_2 &= \begin{pmatrix} B^* & B^{*2} & 0 \\ B^{*2} & B^* & 0 \\ 0 & 0 & B^{*2} \end{pmatrix}. \end{aligned} \quad (45)$$

where $B^* = (\sqrt{5} - 1)/2$.

We iterate eq.44 many times, and estimate $\log \Lambda_1$ by $\log \Lambda_1 \approx \frac{1}{j_{max}} \sum_{j=1}^{j_{max}} \log a_j$. The error in $\log \Lambda_1$ decreases as $\sigma/\sqrt{j_{max}}$, where σ is the rms fluctuation of $\log a_j$. Values of $j_{max} \sim 10^8$ require less than a minute of CPU. For $j_{max} = 10^9$, we find $\sigma \approx 0.45$ and

$$\log \Lambda_1 = -0.23575 \pm 0.00001 \quad (46)$$

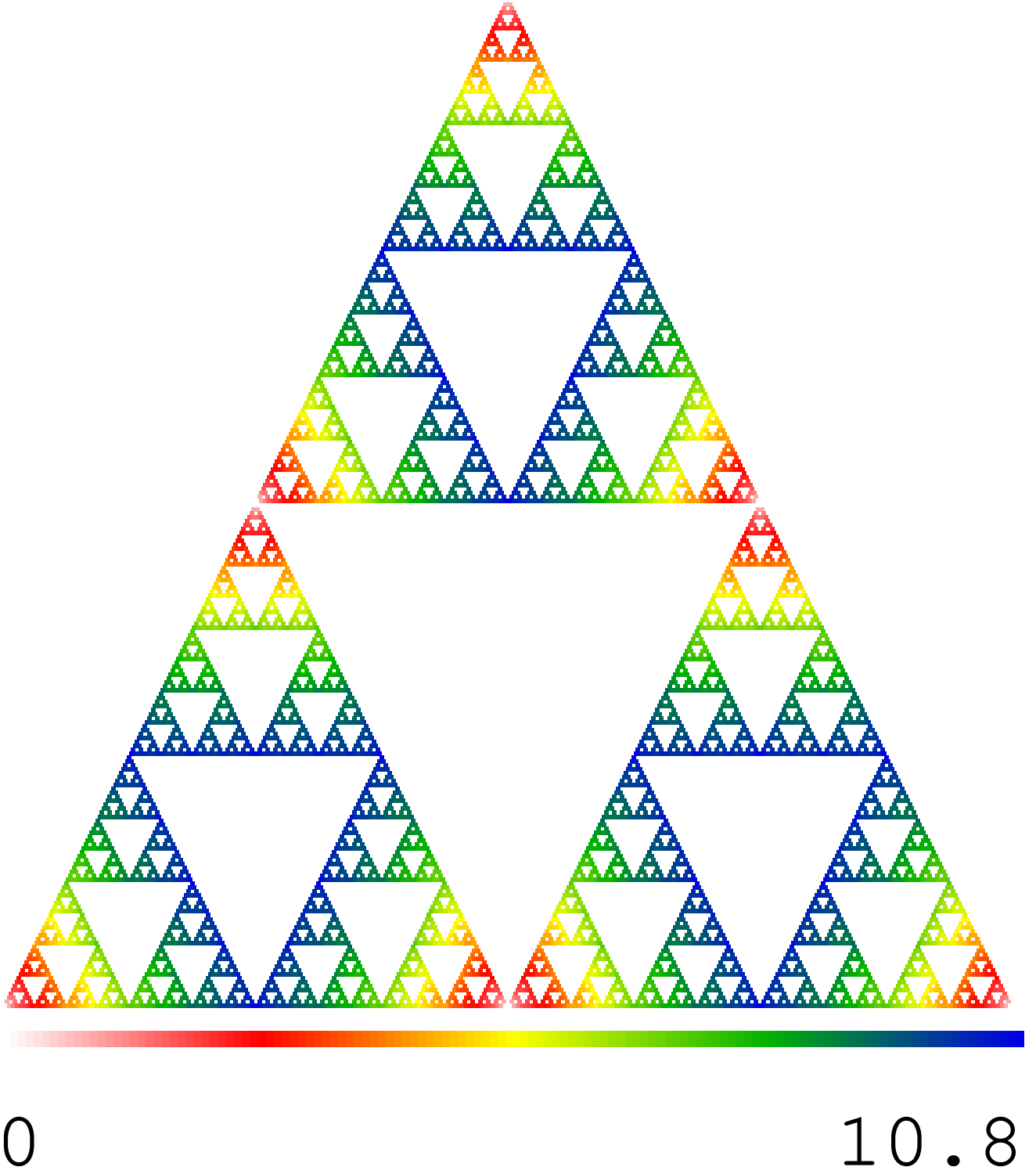


FIG. 9: The plot shows the $\log(P_n(S))$ for $n = 400$ for all sites for fractal lattice upto $r = 9$ generations.

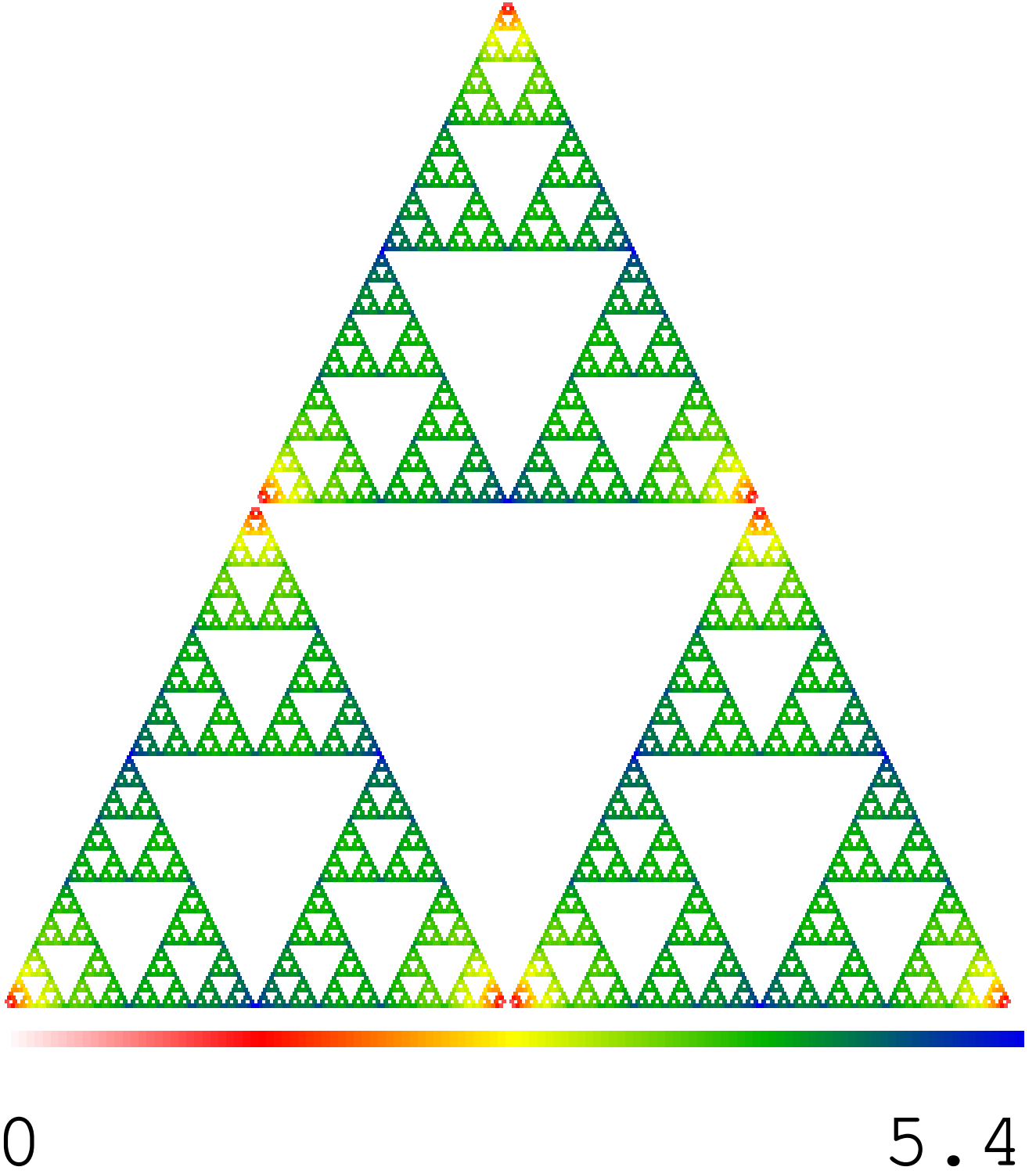


FIG. 10: The plot shows the $\log(P_n(S))$ for $n = 600$ for all sites for fractal lattice upto $r = 9$ generations.

Note that this corresponds to a lattice with $3^{j_{max}}$ sites. This gives $\alpha_q = 0.72837 \pm 0.00001$.

A similar calculation for the exponent γ_q can also be done. To calculate the exponent γ_q , we note that again the most contribution to $W(x; S)$ will come from terms with $r \approx r_0$. At $x = B^*$, $\mathcal{L}_0, \mathcal{L}_1$ and \mathcal{L}_2 become independent of r . If

$$U_{r_0} = \langle u_1 | \mathcal{L}_{s_{r-1}} \dots \mathcal{L}_{s_4} \mathcal{L}_{s_3} \mathcal{L}_{s_2} \mathcal{L}_{s_1} | u_2 \rangle \quad (47)$$

where $\langle u_1 |$ and $| u_2 \rangle$ are 6-dimensional bra- and ket vectors and if $\log \Lambda_2$ is the largest Lyapunov exponent for the random product of matrices,

$$\lim_{r_0 \rightarrow \infty} \frac{1}{r_0} \log U_{r_0} = \log \Lambda_2 \quad (48)$$

Hence, $\log A_i^{(r)}(S)$ and $\log C_i^{(r)}(S)$ will increase as $r \log \Lambda_2$, for almost all S , for $r < r_0$. For $r > r_0$, $A_i^{(r)} \approx A_i^{(r_0)}$ and $C_i^{(r)} \approx 0$. Therefore it follows that the leading order contribution to equation (29) will come from $r = r_0$ term. Hence $\langle \log W_n(S) \mu^{-n} \rangle$ tends to $\log(\lambda_2 \Lambda_2) r_0 - \log(n)$ and we get

$$\gamma_q = \frac{\log(\lambda_2 \Lambda_2)}{\log(\lambda_1)} \quad (49)$$

We find for $j_{max} = 10^9$, $\sigma \approx 1$ and $\Lambda_2 = 1.04845 \pm 0.00003$. Substituting in equation above we get $\gamma_q = 1.37501 \pm 0.00003$.

-
- ¹ K. Barat and B.K. Chakrabarti, *Statistics of Self-avoiding Walk on Random Lattices*, Phys. Rep. 258, 377 (1995)
- ² B. K. Charabarti (ed.), *Statistics of Linear Polymers in Disordered Media*, (Elsevier, Amsterdam, 2005).
- ³ D. Dhar, *Self-avoiding random walks: some exactly soluble cases* J. Math. Phys. **19**, 5-11 (1978).
- ⁴ R. Rammal, G. Toulouse and J. Vannimenus, J. Phys. (Paris) **45**, 389 (1984).
- ⁵ D. Dhar and Y. Singh, in *Statistics of linear polymers in disordered media*, Ed. B. K. Charabarti, (Elsevier, Amsterdam, 2005), p149. [cond-mat/0508330]
- ⁶ Mathematica Wolfram Research <http://www.wolfram.com/>
- ⁷ F. D. A. Reis, *Diffusion on regular random fractals*, J. Phys. A: Math. Gen. **29** (1996) 7803-7810
- ⁸ A. Ordemann, M. Porto and H. E. Roman, *Self-avoiding walks on Sierpinski lattices in two and three dimensions.*, Phys. Rev. E **65** (2002) 021107.
- ⁹ For a mathematical derivation of the log-periodic oscillations in of the Taylor coefficients of functions satisfying functional equations similar to Eq.(28), see A. M. Odlyzko, Adv. Math., **44** (1982) 180. See also, G. Paul, Phys. Rev. **E 59** (1999) 4847; P. J. Grabner and W. Woess, Stochastic Processes and their Applications **69**(1997) 127-138; B Kron and E Teufl, Transactions of the American Mathematical Society **356** (2003) 393-414
- ¹⁰ S. Gluzman and D. Sornette, *Log-periodic route to fractal functions*, Phys. Rev. **E 65** (2002) 036142; D Sornette, *Discrete scale invariance and complex dimensions*, Physics Reports **297** (1998) 239-270
- ¹¹ A. Crisanti, G. Paladin and A. Vulpiani, *Products of Random Matrices in Statistical Physics*, Springer Series in Solid State Sc. **104**(Springer, Berlin, 1993).
- ¹² A. Mukherjee, *Topics in Products of Random Matrices*, (Narosa, New Delhi, 2000).
- ¹³ H. Furstenberg and H. Kesten, Ann. Math. Stat. **31** (1960) 457.
- ¹⁴ T. Halpin-Healy and Y-C Zhang, *Kinetic Roughening, Stochastic Growth, Directed Polymers and all that*, Physics Reports **254**, (1995) 215.

n	$\log \langle P_n \rangle - n \log \mu$	$\langle \log P_n \rangle - n \log \mu$	$\log \langle W_n \rangle - n \log \mu$	$\langle \log W_n \rangle - n \log \mu$
3	-1.4431783323	-1.4442955737	0.3481239636	0.3481239636
7	-2.5207277722	-2.6372273881	0.6327712915	0.5825518549
8	-2.8684082046	-2.8875491290	0.6648211368	0.6276714199
9	-4.3304492827	-4.3328867211	0.6797287773	0.6707214751
15	-4.0919348312	-4.5179887766	0.9155729406	0.8693414702
16	-3.8277310472	-4.0586132570	0.9370278020	0.8829866367
17	-3.7374926267	-3.8857022562	0.9544167885	0.8994169039
18	-3.8145473883	-3.9148386256	0.9693553123	0.9204691093
19	-4.0133264968	-4.0828080387	0.9815329752	0.9429045509
20	-4.3366352924	-4.3875115144	0.9920263470	0.9648015516
40	-4.8957208753	-5.0810665168	1.2742813939	1.2185712350
80	-6.6481626291	-7.2828262546	1.5384807521	1.4965133405
120	-7.0076576021	-7.0786974211	1.6575701703	1.6393667050
160	-9.5287171328	-10.9169115887		
320	-9.6664681509	-9.7339866481		
640	-8.6892637799	-8.7886721125		
768	-10.8851067629	-10.9571396026		

TABLE I: Values of quenched and annealed averages for SAP and SAW for some representative values of n .